19

Surface plasmon polaritons in ordered arrays of metallic carbon nanotubes with dielectric filling

© V.A. Zaytsev[1], S.A. Afanasev[1], S.G. Moiseev[1,2], I.A. Rozhleys[1], D.G. Sannikov[1,¶], A.V. Sysa[1,3], Yu.P. Shaman[1,3]

[1] Ulyanovsk State University,
Ulyanovsk, Russia
[2] Kotelnikov Institute of Radio Engineering and Electronics of Russian Academy of Sciences, Ulyanovsk branch,
Ulyanovsk, Russia
[3] Scientific-Industrial Complex „Technology Center",
Moscow, Russia

[¶] e-mail: sannikov-dg@yandex.ru

Received April 30, 2025
Revised July 12, 2025
Accepted October 24, 2025

The dispersion characteristics of surface plasmon polaritons (SPPs) in the terahertz frequency range are studied in ordered arrays of single- and double-walled carbon nanotubes immersed in a dielectric medium. Dispersion relations for SPPs in an isolated nanotube with a dielectric environment were obtained analytically and then used to verify the solutions obtained by numerical simulation. Frequency dependences of the propagation and attenuation constants, as well as the SPP deceleration coefficient, are obtained for arrays of different densities by numerical simulation. It is found that in dense CNT arrays, the propagation constants and the mean free path of SPPs are smaller than in isolated nanotubes. The deceleration coefficient increases with increasing nanotube diameter and permittivity of the host medium.

Keywords: single- and double-walled carbon nanotubes, dense nanotube array, surface plasmon polaritons, surface wave deceleration.

DOI: 10.61011/EOS.2025.10.62564.7957-25

Introduction

To date, various technologies have been developed for obtaining ordered arrays of carbon nanotubes (CNTs) with controlled parameters [1,2]. One method to improve the functional characteristics of such arrays is to embed CNTs in a transparent dielectric matrix made of polymeric materials [3,4]. These structures hold significant practical interest for the generation and control of electromagnetic radiation. In particular, CNTs can support the propagation of ultraslow (with phase velocity two orders of magnitude lower than the speed of light in vacuum) surface plasmon polaritons (SPPs) [5,6]. Under conditions where the SPP phase velocity is close to the drift velocity of free charge carriers, the interaction of the surface wave with the current flowing along the CNT walls can lead to its amplification [7]. Based on this effect, compact sources of coherent terahertz radiation can be developed [8]. The present work investigates the dispersion characteristics of terahertz SPPs in arrays of single-walled (SWCNT) and double-walled (DWCNT) CNTs, accounting for ohmic losses and the presence of surrounding dielectric medium As the baseline model, an ordered array of parallel nanotubes with identical parameters is selected.

Dispersion equation for surface plasmon polaritons in single-walled and double-walled isolated nanotubes

Solving the waveguide electrodynamic problem yields the dispersion relation linking the SPP frequency ω with its propagation constant (PC) for isolated nanotubes. To begin, consider the more general case of a double-walled nanotube (DWCNT).

The DWCNT model consists of a system of two coaxial cylinders with radii a_1 and $a_2 > a_1$ and a typical wall separation of 0.34 nm. The DWCNT length is $L \gg a_{1,2}$ so the nanotube is treated as infinitely long. The problem is solved in the cylindrical coordinate system (r, φ, z), where r is the radial coordinate, φ is the azimuthal angle, and z is the coordinate axis directed along the DWCNT symmetry axis. The regions inside $(r < a_1)$ and outside $(r > a_2)$ the nanotube are, in general, filled with transparent dielectrics having permittivities ε_1 and ε_2 respectively.

In this work, the analysis is limited to the fundamental SPP mode, for which the field components are independent of the azimuthal angle φ. In the terahertz frequency range, this mode has no cutoff and is characterized by low attenuation coefficients (propagation lengths on the order of micrometers) [8,9]. The DWCNT walls are electrically conductive and characterized by the surface conductivity

tensor $\hat{\sigma}_j$ ($j = 1, 2$ is the wall number), whose axial component takes the form [6]:

$$\sigma^{(0)}_{zz,j} = \sigma_0 \omega \tilde{\omega} / \Omega, \qquad (1)$$

where $\sigma_0 = 2iV_F e^2/(\pi^2 \hbar a_j \tilde{\omega})$, $\Omega = \omega\tilde{\omega} - V_F^2 q^2/2$, q is the PC of the surface wave, $\tilde{\omega} = \omega + i\tau^{-1}$, τ is the relaxation time, V_F is the Fermi velocity ($V_F = 10^6$ m/s), e is the elementary charge, and $\hbar$ is the Planck constant. Expression (1) accounts for dissipative losses and spatial dispersion of SPPs in CNTs [6].

To find the guided modes in an isolated DWCNT, the waveguide electrodynamic problem is solved subject to boundary conditions at its walls. The solutions to the Helmholtz equation for the fundamental mode are expressed in terms of zero-order modified Bessel functions I_0 and K_0. In the approximation $q \gg k_0$ ($k_0 = \omega/c$, c is the speed of light in vacuum), the determinant equation for this mode takes the form:

$$\det\begin{pmatrix} \Omega M_{11} - \omega_{p1}^2 (qa_1) I_0^2 (qa_1) & \Omega M_{12} - \omega_{p1}^2 (qa_1) K_0 (qa_1) I_0 (qa_1) \\ \Omega M_{21} - \omega_{p2}^2 (qa_2) I_0 (qa_2) K_0 (qa_2) & \Omega M_{22} - \omega_{p2}^2 (qa_2) K_0^2 (qa_2) \end{pmatrix} = 0, \qquad (2)$$

where $\omega_{pj}^2 = 2V_F e^2/(\pi^2 \hbar \varepsilon_0 a_j^2)$ is the square of the plasma frequency for the wall of radius a_j,

$$M_{12} = \varepsilon_1 K_0(qa_1) I_0'(qa_1) - I_0(qa_1) K_0'(qa_1),$$

$$M_{21} = K_0(qa_2) I_0'(qa_2) - \varepsilon_2 I_0(qa_2) K_0'(qa_2),$$

$M_{11} = (\varepsilon_1 - 1) I_0(qa_1) I_0'(qa_1)$,
$M_{22} = (1 - \varepsilon_2) K_0(qa_2) K_0'(qa_2)$, ε_0 is the permittivity of free space. Equation (2) reduces to a biquadratic equation in frequency ω, whose two positive roots correspond to the two branches of the dispersion relation for SPPs in DWCNTs — the high-frequency (HF) and low-frequency (LF) branches.

Analogously, the simpler case of an isolated nanotube with a single cylindrical wall of radius a and conductivity of form (1) can be analyzed. Unlike the DWCNT case, the dispersion relation for SWCNTs contains only one dispersion branch, described by

$$\omega\tilde{\omega} = V_F q^2/2 + \omega_p^2 qa I_0(qa) K_0(qa)/C. \qquad (3)$$

The parameter $C = C_1 + C_2$ is positive, since at $\varepsilon_{1,2} > 0$, $C_1 = \varepsilon_1 I_0'(qa) K_0(qa) > 0$, $C_2 = -\varepsilon_2 I_0(qa) K_0'(qa) > 0$. Analysis of equation (3) shows that, at fixed q increasing ε_1 or ε_2 decreases the SPP frequency ω and, consequently, increases the deceleration factor $K_{dec} = q'/k_0 = q'c/\omega$, where q' is the real part of the SPP PC. At a given frequency ω the value of K_{dec} is minimal at $\varepsilon_1 = \varepsilon_2 = 1$, i.e., for the case of SWCNTs in air. It should be noted that at terahertz frequencies, the term C_1 is negligible compared to C_2, and since $C_1 \sim \varepsilon_1$ and $C_2 \sim \varepsilon_2$, the optical properties of the material inside the SWCNT have virtually no effect on the SPP dispersion characteristics.

Dispersion characteristics of surface plasmon polaritons in arrays of single-walled and double-walled nanotubes

Consider an infinite ordered array of SWCNTs with a square unit cell, in which the centers of neighboring nanotubes are equidistant at separation d (array period). To calculate the SPP dispersion characteristics, we employ electrodynamic modeling via the finite element method, as implemented in the Comsol Multiphysics software package. For the unit cell with side d containing one nanotube, periodic boundary conditions are applied, accounting for the influence of neighboring nanotubes on the SPP characteristics.

The computational modeling results are presented in Fig. 1 as dependencies of the real and imaginary PC components $q = q' + iq''$ of the fundamental SPP mode on the array period d. The dependencies are plotted for SWCNT arrays in different embedding media (air, polyethylene) at several terahertz-range frequencies with $\tau = 10^{-12}$ s [10]. Invalid inter-particle distances d (less than the nanotube outer diameter $2a$) are shown as shaded regions on the left side of the plots. Here and below, the following normalization parameters are used: $a_0 = 1$ nm, $\omega_0 = (e/\pi a_0)(2V_F/\varepsilon_0\hbar)^{1/2} \approx 2.36 \cdot 10^{15}$ s^{-1}.

The presented dependencies show that for rare-field arrays ($d \gg 2a$) the PC is nearly independent of the SWCNT separation, as surface electromagnetic waves on even neighboring nanotubes interact weakly, so their dispersion characteristics remain the same as for isolated nanotubes. In this case, the numerical solutions shown in Fig. 1 coincide with the analytical solutions of equation (3) obtained for isolated SWCNTs.

In the case of dense arrays, for which $d < 2(a + \Delta)$, where $\Delta \approx 2/q'$ is the decay length scale of the evanescent field outside the nanotube, a change in the SPP dispersion characteristics is observed. The inset in Fig. 1, *a* illustrates the transformation of the fundamental mode in the SWCNT array as its density increases, manifesting as the formation of a „petal-like“ structure (azimuthal dependence) in the wave field distribution. As d decreases, the real part of the PC decreases and the imaginary part increases, indicating a reduction in the SPP deceleration factor and propagation length.

Fig. 1 also shows that the presence of an embedding medium with $\varepsilon_2 > 1$ leads to an increase in both the real and imaginary (except in a very narrow range of periods d near the cutoff for the nanotube array in air at the same SPP frequency) parts of the SPP PC, as well as an extension (toward smaller values) of the range of d, for which SPPs can exist in the SWCNT array.

Dispersion dependencies of the PC and deceleration factor K_{dec} for the fundamental SPP mode in SWCNT and DWCNT arrays, as well as in isolated nanotubes (the case $d \to \infty$) are presented in Fig. 2. First and foremost, we note the common features of these dependencies for both types of nanotubes. In dense arrays,

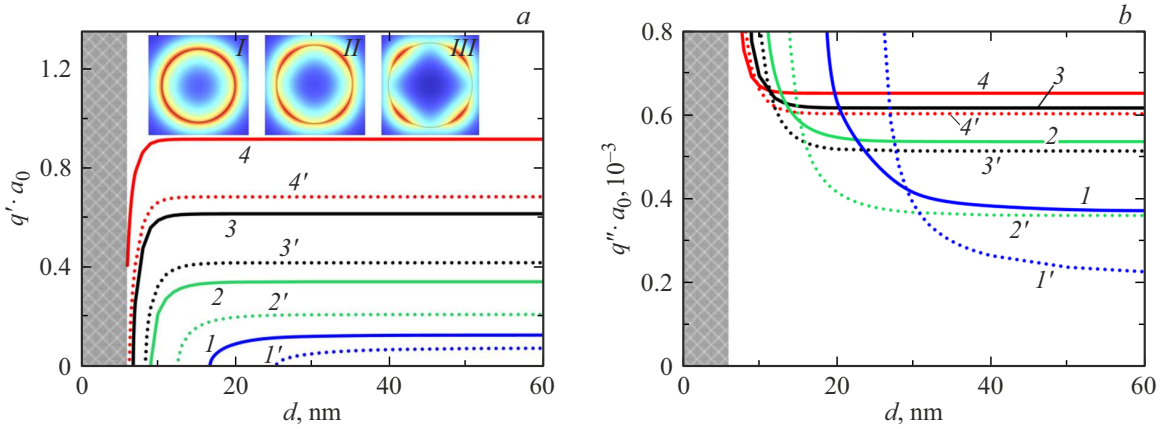

Figure 1. Dependencies of the real (a) and imaginary (b) parts of the PC components of the fundamental SPP mode on the SWCNT array period for different dielectric permittivities of the media: $\varepsilon_1 = \varepsilon_2 = 1$ (air) — dashed curves $1'–4'$, $\varepsilon_1 = 1$ and $\varepsilon_2 = 4$ (polyethylene) — solid curves $1–4$. Curve pairs 1 and 1′, 2 and 2′, 3 and 3′, 4 and 4′ correspond to frequencies $(0.1, 0.2, 0.3, 0.4)\omega_0$ respectively. SWCNT radius $a = 3$ nm. Inset in panel (a): magnitude of the electric field of the fundamental mode at frequency $0.4\omega_0$ at $d = 10$ nm (I), 9 nm (II), 8 nm (III).

there are low-frequency cutoff regions (curves $2–4$ and $2'–4'$), which are absent in the case of isolated nanotubes (curves 1 and $1'$). In the presence of an embedding medium with $\varepsilon_2 > 1$ the frequency range of SPP existence expands, while the deceleration factor and propagation length of SPPs decrease (except in a narrow frequency range near the cutoff frequency for the nanotube array in air).

Dispersion dependencies for DWCNT arrays (Fig. 2, $d–f$) exhibit features associated with the presence of two dispersion branches. For the HF branch, the dispersion properties of SPPs are analogous to those observed in SWCNT arrays; however, the deceleration factor of the surface wave in the DWCNT array takes significantly smaller values. The LF branch of the fundamental mode is characterized by a high degree of field localization in the region between the nanotube walls, which results in weak sensitivity of its dispersion characteristics to the array density and the dielectric permittivity of the surrounding medium. The field localization of the mode inside the nanotube also leads to the absence of cutoff in dense arrays almost up to the minimum possible period value $d \approx 2a$. The LF branches are characterized by significantly higher deceleration ($K_{\text{dec}} > 300$ in the frequency range considered), but shorter propagation lengths compared to both the SWCNT array mode and the HF branch of the DWCNT array.

Conclusion

Numerical modeling of SPP dispersion characteristics in dense ordered arrays of SWCNTs and DWCNTs has been performed, accounting for the mutual influence of electromagnetic fields from the nanotubes. The dispersion equation for SPPs in isolated nanotubes has been derived analytically, taking into account the dielectric permittivity of the surrounding medium. For sparse arrays of CNTs agreement between numerical and analytical calculations has been demonstrated. It has been established that in dense nanotube arrays, interaction via evanescent fields leads to a decrease in the PC and propagation length, as well as the emergence of a frequency cutoff for the fundamental SPP mode. It has also been shown that in the presence of an embedding dielectric medium, the SPP phase velocity decreases, and SPPs can be excited in denser nanotube arrays. In the DWCNT array, the LF branch of the fundamental mode demonstrates weak sensitivity to both the array density and the properties of the embedding medium, while the HF branch proves sensitive to changes in the electrodynamic characteristics of the surrounding medium. The results of this study may be useful for designing sensors, modulators, and SPP generators based on CNT arrays with drift current pumping.

Funding

This research was supported by the Russian Science Foundation (grant № 23-19-00880).

Conflict of interest

The authors declare that they have no conflict of interest.

References

[1] Z.J. Dong, B. Sun, H. Zhu, G.M. Yuan, B.L. Li, J.G. Guo, X.K. Li, Y. Cong, J. Zhang. New Carbon Mater., **36** (5), 873 (2021). DOI: 10.1016/S1872-5805(21)60090-2

[2] M. He, S. Zhang, J. Zhang. Chem. Rev., **120** (22), 12592 (2020). DOI: 10.1021/ACS.CHEMREV.0C00395

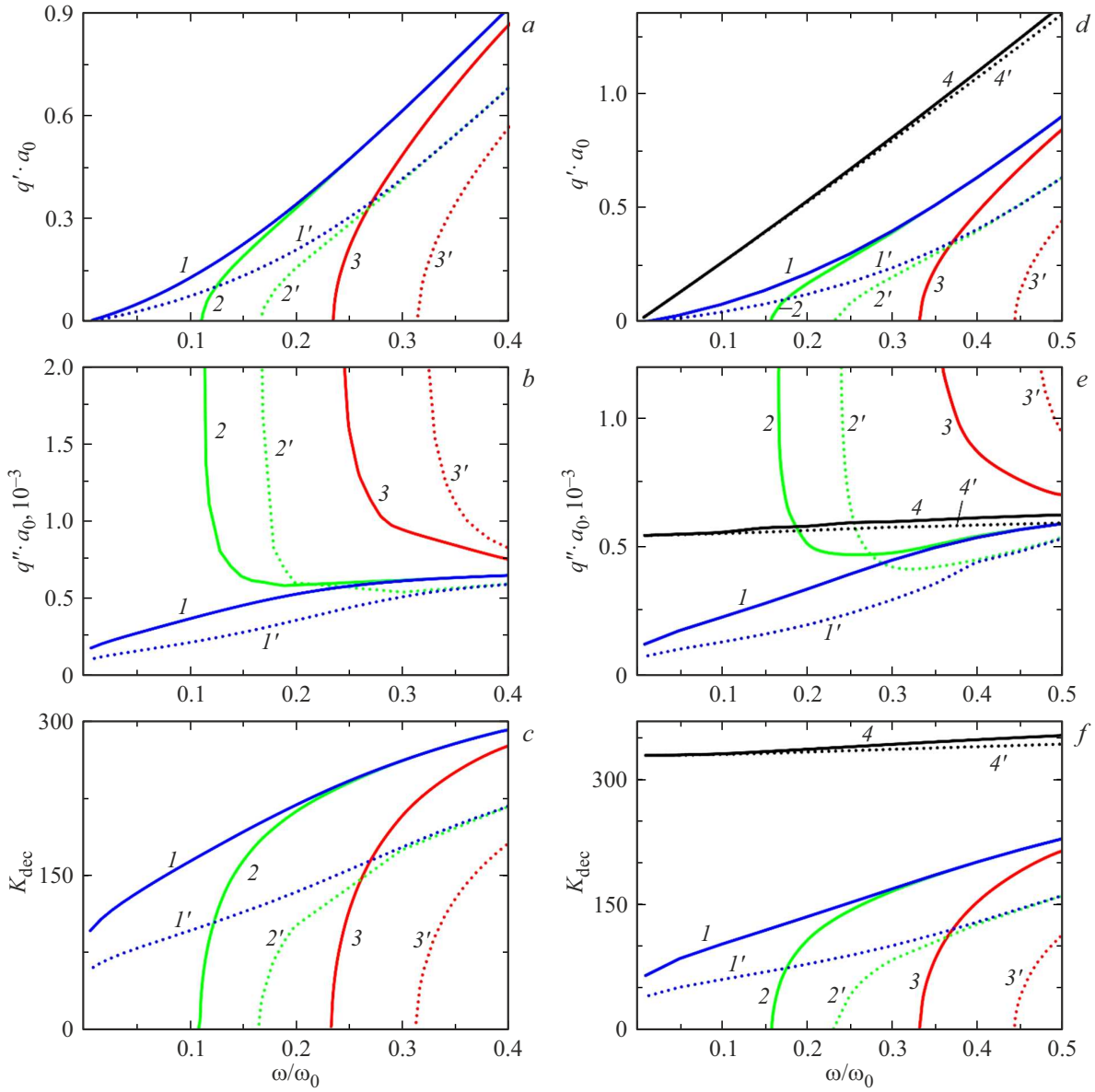

Figure 2. Dispersion dependencies of the real (*a, d*), imaginary (*b, e*) PC components and deceleration factor (*c,f*) for the fundamental SPP mode in SWCNT (*a, b, c*) and DWCNT (*d, e, f*) arrays for different dielectric permittivities of the media: $\varepsilon_1 = \varepsilon_2 = 1$ — dashed curves *1′–4′*, $\varepsilon_1 = 1$ and $\varepsilon_2 = 2.4$ — solid curves *1–4*. For the SWCNT array: dependencies for $d = (\infty,\ 15,\ 8)$ nm are shown by curve pairs *1* and *1′*, *2* and *2′*, *3* and *3′* respectively. For the DWCNT array: HF branches for $d = (\infty, 15, 8)$ nm are shown by curve pairs *1* and *1′*, *2* and *2′*, *3* and *3′* respectively; LF branches for $d = 8$ nm — curves *4* and *4′*. SWCNT radius $a = 3$ nm. DWCNT wall radii $a_1 = 2.66$ nm, $a_2 = 3$ nm.

[3] P.S. Goh, A.F. Ismail, B.C. Ng. Composites Part A: Applied Science and Manufacturing, 56, 103 (2014). DOI: 10.1016/j.compositesa.2013.10.001
[4] K. Silakaew, P. Thongbai. RSC Adv., **9** (41), 23498 (2019). DOI: 10.1039/c9ra04933a
[5] G.Y. Slepyan, S.A. Maksimenko, A. Lakhtakia, O. Yevtushenko, A.V. Gusakov. Phys. Rev. B, **60** (24), 17136 (1999). DOI: 10.1103/PhysRevB.60.17136
[6] A. Moradi. Appl. Phys. A: Mater. Sci. Process., **113** (1), 97 (2013). DOI: 10.1007/s00339-013-7854-5
[7] A.S. Kadochkin, S.G. Moiseev, V.V. Svetukhin, A.N. Saurov, I.O. Zolotovskii. Ann. Phys., **534** (4), 2100438 (2022). DOI: 10.1002/ANDP.202100438
[8] S.A. Afanas'ev, A.A. Fotiadi, A.S. Kadochkin, E.P. Kitsyuk, S.G. Moiseev, D.G. Sannikov, V.V. Svetukhin, Y.P. Shaman, I.O. Zolotovskii. Photonics, **10** (12), 1317 (2023). DOI: 10.3390/PHOTONICS10121317
[9] S.A. Afanas'ev, V.A. Zaitsev, S.G. Moiseev, I.A. Rozhleis, D.G. Sannikov, G.V. Tertyshnikova. FTP, **58** (9), 467 (2024) (in Russian). DOI: 10.61011/FTP.2024.09.59302.6326A
[10] R.A. Jishi, M.S. Dresselhaus, G. Dresselhaus. Phys. Rev. B, **47** (24), 16671 (1993). DOI: 10.1103/PhysRevB.47.16671

Translated by J.Savelyeva